European Journal of Medicinal Chemistry 46 (2011) 1165–1171

Contents lists available at ScienceDirect

European Journal of Medicinal Chemistry

journal homepage: http://www.elsevier.com/locate/ejmech

Original article

Structure–activity relationship of 2,4,5-trioxoimidazolidines as inhibitors of thymidine phosphorylase

Mehdi Rajabi, David Mansell, Sally Freeman*, Richard A. Bryce**

School of Pharmacy and Pharmaceutical Sciences, University of Manchester, Oxford Road, Manchester M13 9PT, UK

ARTICLE INFO

Article history:
Received 3 August 2010
Received in revised form
14 October 2010
Accepted 22 January 2011
Available online 31 January 2011

Keywords:
Thymidine phosphorylase
Trioxoimidazolidine
Parabanic acid
Hydantoin
Anti-angiogenic
Molecular modelling

ABSTRACT

Novel non-nucleobase-derived inhibitors of the angiogenic enzyme, thymidine phosphorylase, have been identified using molecular modelling, synthesis and biological evaluation. These inhibitors are 2,4,5-trioxoimidazolidines bearing *N*-(substituted)phenylalkyl groups, together with, in most cases, *N*′-$(CH_2)_n$-carboxylic acid, ester or amide side chains. The best compound from this series is 3-(2,4,5-trioxo-3-phenylethyl-imidazolodin-1-yl)propionamide, with an IC_{50} of 40 μM against *Escherichia coli* TP. Molecular modelling suggests that this ligand, when complexed with closed-cleft human TP, would have the phenylalkyl group in the active site region normally occupied by a thymine-containing structure.

1. Introduction

Thymidine phosphorylase (TP, dThPase, E.C. 2.4.2.4), also known as the platelet-derived endothelial cell growth factor (PD-ECGF), catalyses the phosphorolysis of thymidine (**1**) to 2-deoxyribose-1-phosphate (**2**) and thymine (**3**) (Fig. 1) [1]. TP is highly expressed in many solid human tumours, facilitating tumour growth by promoting angiogenesis, metastasis and suppressing apoptosis [2–5].

Furthermore, intracellular hydrolysis of **2** generates 2-deoxy-D-ribose [6] which promotes angiogenesis, the chemotactic activity of endothelial cells and also confers resistance to hypoxia-induced apoptosis in some cancer cell lines [2,7]. Thus, TP is considered an attractive therapeutic target for inhibition of tumour angiogenesis and concomitant tumour growth and metastasis [5].

Almost all literature TP inhibitors are based on uracil or very closely related ring systems. One of the most potent inhibitors, 5-chloro-6-[1-(2-iminopyrrolidinyl)methyl]uracil hydrochloride (**4**, TPI, Fig. 2), caused a reduction in the rate of tumour growth when administered to mice carrying tumours that over-expressed human TP [8]. Prodrugs of inhibitors of TP have also been synthesised in which 2-nitroimidazolyluracil prodrugs (**5A**) require bioactivation under tumour conditions to form the active species, 2′-amino-imidazolyluracils (**5B**) (Fig. 2) [9–11], one of which demonstrated activity similar to TPI (apparent IC_{50} 0.023 μM against human TP) [10,11]. These zwitterionic tight-binding inhibitors are proposed to mimic parts of the oxacarbenium ion-like transition state formed during thymidine phosphoroylsis, see Fig. 1 [12]. Despite the potency levels of these inhibitors, their highly ionic nature and poor pharmacokinetic profiles remain as substantial limitations.

Recently, novel scaffolds for TP inhibitors have been targeted with the aid of 3D-homology models of human pyrimidine nucleoside phosphorylase and *Escherichia coli* TP [12,13]. We have previously employed structure-based virtual screening of the National Cancer Institute (NCI) database against the open conformation of the homology model of human TP [9] based on a crystal structure of the *E. coli* enzyme [13]. This study identified hydantoin **7** (Fig. 3) as a TP inhibitor lead with micromolar activity against human and *E.coli* TP [13], comparable to that of the known, non-uracil-based TP inhibitor, 7-deazaxanthine (**6**). This novel scaffold lacks the undesirable ionic sites of the existing tight-binding nucleobase-derived inhibitors and therefore may possess improved pharmacokinetic and cell-penetrating properties.

Based on our knowledge of this hydantoin (2,4-dioxoimidazolidine) lead, we here employ molecular modelling, synthesis and biological assays to identify further active non-nucleoside lead scaffolds as a basis for development of novel TP inhibitors.

* Corresponding author. Tel.: +44 161 275 2366; fax: +44 161 275 2396.
** Corresponding author. Tel.: +44 161 275 8345; fax: +44 161 275 2396.
E-mail addresses: Sally.Freeman@manchester.ac.uk (S. Freeman), Richard.Bryce@manchester.ac.uk (R.A. Bryce).

0223-5234/$ – see front matter © 2011 Elsevier Masson SAS. All rights reserved.
doi:10.1016/j.ejmech.2011.01.035

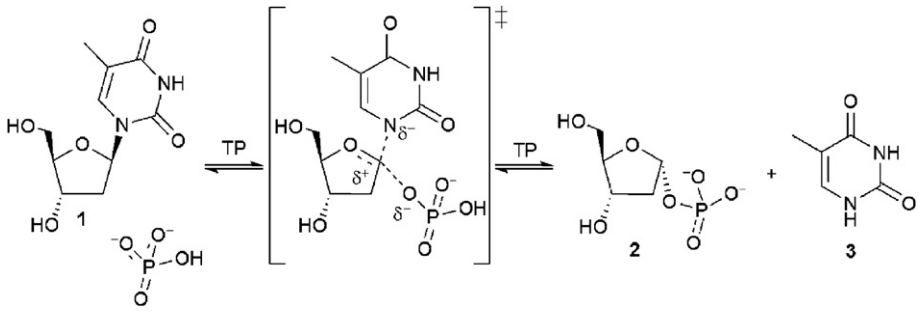

Fig. 1. Phosphorolysis of thymidine (**1**) to 2-deoxyribose-1-phosphate (**2**) and thymine (**3**).

2. Results and discussion

In an initial modelling step, the NCI and Available Chemicals Directory (ACD) databases were filtered to identify all imidazolidine-containing compounds [14]. The identified compounds were then screened *in silico* against an X-ray structure of closed-cleft human TP [15], in which phosphate was modelled into the active site; these compounds were ranked according to calculated docking scores [14]. Interestingly, the top-ranked NCI ligand from this screen was the hydantoin, 4-hexyl-1-methyl-2,5-dioxo-4-imidazolidinecarbaldehyde semicarbazone (**8**). This ligand is very similar to the previously identified hydantoin derivative **7** [13], the only difference being the presence of an extra methylene group in the aliphatic chain. The top-ranked ACD ligand from the screen was [3-(2-methylbenzyl)-2,4,5-trioxo-imidazolidin-1-yl]ethanoic acid (**9**). Its complex with TP was predicted to be more stable (by 36.4 kJ/mol) than that of compound **8** [14].

2.1. Chemistry

Based on this predicted preference of imidazolidines for the active site of TP, the chemical space surrounding the highest scoring compound, **9**, was explored: a series of 3-arylalkyl-2,4,5-trioxoimidazolidine-1-ethanoic acids (parabanic acid derivatives), including **9**, and their corresponding esters and amides were prepared (Scheme 1) and tested for their TP inhibitory activities (Table 1). We note that some of these compounds have previously been investigated for their therapeutic potential for reduction of diabetic complications such as neuropathy, nephropathy, retinopathy, keratopathy, angiopathy and cataracts by selectively inhibiting the enzyme aldose reductase [16–18].

The general synthetic route for the acids and their esters is shown in Scheme 1 and is based on chemistry developed by Ishii and coworkers [19]. The synthesis starts from benzylamine derivatives **10**–**13**, which are reacted with urea in the presence of acid to yield *N*-(benzyl)urea derivatives **14**–**17**. Treatment of the *N*-(benzyl)urea derivatives **14**–**17** with oxalyl chloride gave the 1-(benzyl)-imidazolidine-2,4,5-triones **18**–**21** in good yields. The ethyl [3-benzyl-2,4,5-trioxo-imidazolidin-1-yl]ethanoates **22**–**25** were then prepared by reaction of **18**–**21** with ethyl bromoethanoate in the presence of potassium hydroxide. Acid-catalysed hydrolysis of esters **22**–**25** gave the 3-benzyl-2,4,5-trioxo-imidazolidin-1-yl-ethanoic acids **9** and **26**–**28** in good yields. The novel amide analogues **29**–**32** were obtained by reaction of the imidazolidine-2,4,5-trione derivatives **18**–**21** with 3-bromopropionamide (Scheme 1). Amides **29**–**32** were fully characterized by ^{1}H and ^{13}C NMR spectroscopy, elemental analysis and mass spectrometry.

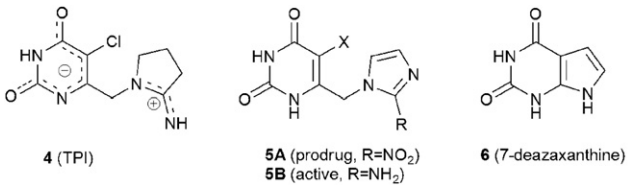

Fig. 2. Examples of known TP inhibitors.

2.2. Structure–activity relationship

Compound **9** and **18**–**32** were tested for their TP inhibitory activity using *E. coli* TP. A spectrophotometric assay was used to measure the decrease in absorbance (at 265 nm) of the natural substrate thymidine upon the addition of the compounds [10,20]. The experimental IC_{50} values are presented alongside their calculated docking scores in Table 1, together with the data for the inhibitor TPI (**4**) as a positive control.

The data presented in Table 1 for the 1-arylalkyl-2,4,5-trioxoimidazolidines (**18**–**21**) indicate that there is little difference in TP inhibition activity between these compounds. This indicates that the nature of substituent, X, on the phenyl ring has a rather weak influence on the overall binding affinity of the ligands. Correspondingly, these groups do not appear to interact directly with the protein in the predicted binding poses. This is also evident from their similar calculated energy scores. Indeed, compounds **18**–**21** all bind in very similar conformations with good interactions formed between the imidazolidine-2,4,5-trione ring and Ser217 and Arg202 residues, with the phenyl ring located in the centre of the active site.

Ligands **22**–**32** examine the effect of the presence of side chains opposite the lipophilic aryl substituent (Table 1). The ester groups in ligands **22**–**25** constitute hydrogen bond acceptors and the ethyl groups have the ability to make lipophilic interactions. The presence of the ester functionality generally decreased TP inhibition when compared with other analogues in Table 1. Replacing the ester functional group with the carboxylic acid group led to a marked improvement in the calculated GoldScore value, comparable to the value obtained for TPI (Table 1). The most stable binding conformation predicted for compound **9**, which was the top-ranked ligand in the original screen of the ACD database and displayed the highest calculated score (−72.2 kJ/mol) of all the

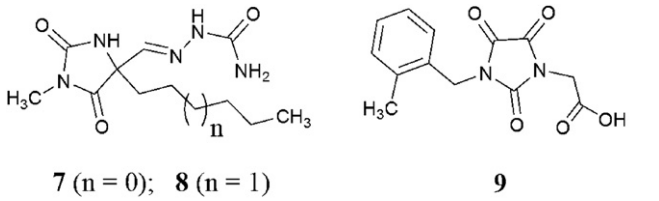

Fig. 3. Hydantoins **7** and **8** and trioxoimidazolidine **9** were TP inhibitors identified by *in silico* screening of NCI and ACD databases.

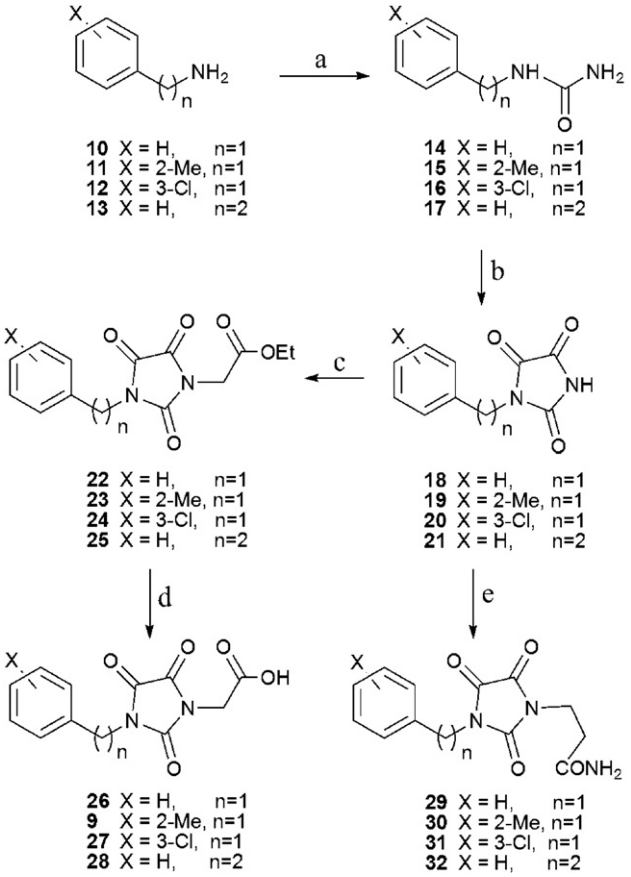

Scheme 1. Synthesis of 2,4,5-trioxoimidazolidin-1-yl derivatives (**9** and **18**–**32**): (a) Urea, HCl, Δ; (b) Oxalyl chloride, THF; (c) Ethyl bromoacetate, KOH, EtOH, Δ; (d) Acetic acid, HCl, Δ; (e) 3-Bromopropionamide, KOH, EtOH, Δ.

ligands in this study, is shown in Fig. 4 and is representative of the other carboxylic acids derivatives (**26**–**28**). The carboxylate functionality appeared to form strong interactions with the Arg202 and Ser217 residues (Fig. 4), the same region with which TPI interacts. Consequently, these ligands and in particular compound **9**, would be predicted to possess the most potent TP inhibition activity. However, the novel amide derivatives (**29**–**32**) generally displayed better IC_{50} values compared to other ligands in the study, with the IC_{50} values obtained for **31** and **32** being comparable to 7-deazaxanthine [21]. Amongst the carboxylate and amide derivatives, the ligands for which $n = 1$ (eg. **29**–**31** for the amides) appear to be too short to effectively span the active site, from Arg202 to Asp123. In contrast, ligands **28** and **32**, where $n = 2$, appear to have the dimensions to achieve this. The greater level of interaction for $n = 2$ compounds is illustrated by the 2-fold difference in potency for compounds **29** and **32**; or for the carboxylate series, by the 3-fold difference between compounds **26** and **28**.

The superior experimental inhibitory effect exhibited by the amide derivatives was not reflected in the predicted values obtained for their binding energy. Interestingly however, the predicted top-scoring binding orientation of compound **32**, the most potent inhibitor of all the compounds studied (Fig. 5), was inverted with respect to the carboxylate-containing compounds (Fig. 4): in this case, the phenyl ring was positioned upwards towards the hydrophobic pocket at the top of the active site due to interactions formed between the amide group and (i) the Asp123 residue (ligand N–H···O Asp123 backbone distance of 1.8 Å, Fig. 5), and (ii) the phosphate hydroxyl group at the bottom of the active site. In addition, a strong interaction was observed between the 5-oxo group on the imidazole ring and the Thr154 residue at the centre of the active site (O···H–N backbone distance of 1.9 Å, Fig. 5). This orientation was also observed in compound **29**, but not in amides **30** and **31**, which possess bulkier substituted phenyl rings. Therefore, the top-ranked docking pose would suggest that the interaction between the amide functionality in **29** and **32** with the Asp123 and Thr145 drives the flip in binding orientation, whereas in **30** and **31** this orientation is energetically unfavourable due to the increased steric bulk on the phenyl ring. Summarising, in the amide series, substitution on the phenyl ring appears to have a more significant influence on the predicted binding orientation of the ligand, when compared with either the ester or carboxylic acid derivatives.

3. Conclusions

In silico screening of the NCI and ACD databases identified several inhibitors of human TP [14]. From this, a series of 3-arylalkyl-2,4,5-trioxoimidazolidine-1-ethanoic acids (parabanic acid derivatives) and their corresponding esters and amides (Table 1) were prepared and their biological activity evaluated against *E.coli* TP. In this series, compounds **32**, **31** and **28** showed the greatest *E.coli* TP inhibition with IC_{50} values of 40, 66 and 85 μM, respectively. These inhibitors are unrelated to the molecular framework of the thymine substrate or any previously reported ligands, and therefore constitute a new direction for design and synthesis of novel TP inhibitors with potentially improved pharmacokinetic and cell-penetrating properties.

4. Experimental

4.1. Molecular modelling

All docking/screening studies employed the X-ray crystal structure of human TP in complex with the inhibitor TPI (**4**) and in the absence of phosphate (resolution 2.1 Å, PDB code 1UOU) [15]. TPI was removed and positioning of the active site phosphate molecule was performed *via* analogy with the crystal structure of *Bacillus stearothermophilus* pyrimidine nucleoside phosphorylase (PyNP), in which the phosphate group is present [22]. The location of hydrogen atoms was modelled into the structure using SYBYL 6 (Tripos Inc.: St Louis, MO, USA 2003). The phosphate was modelled in its dihydrogen form. We note that *in silico* docking of TPI reproduced its crystallographically observed binding mode [15]: the nucleobase interacted *via* hydrogen bonds with residues including His116 (not shown), Ser217, Arg202 and Lys221. This is the region of the active site that binds the nucleobase of the thymidine substrate. TPI's chloro-substituent projected into a lipophilic pocket formed by residues Leu148, Val208, Ile214 and Val241; the cationic NH_2 group of the aminopyrrolidinium ring interacted with the carbonyl oxygen of Ser117 and an oxygen atom of the phosphate co-ligand. Three-dimensional structures of ligands **9** and **18**–**33** were assigned using ViewerLite (Accelrys Software Inc.). Compounds **9** and **26**–**28** were modelled as their carboxylate anions. Initial screening of the NCI and ACD databases was performed using flexible ligand docking *via* the program DOCK4 [23] using Gasteiger-Marsili partial charges for the protein atoms [24] and ligand atomic charges consistent with the MMFF94s force field [25]. Subsequent analysis of structure–activity data was performed using GOLD and the GoldScore scoring function [26].

4.2. Instrumentation and chemicals

NMR spectra were recorded on a Bruker Avance 300 MHz spectrometer. ^1H and ^{13}C NMR spectra were reported as δ_H parts per million (ppm) downfield from tetramethylsilane. The ^{13}C NMR

Table 1
Interaction energies and *E. coli* TP inhibition data for 1-arylalkyl-2,4,5-trioxoimidazolodine analogues (**18**–**21**), and 1-arylalkyl-3-substituted-2,4,5-trioxoimidazolodine esters (**22**–**25**), carboxylic acids (**9** and **26**–**28**) and amides (**29**–**32**). Docking scores are calculated using GoldScore (kJ/mol).

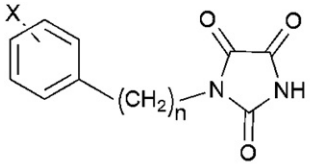

18-21

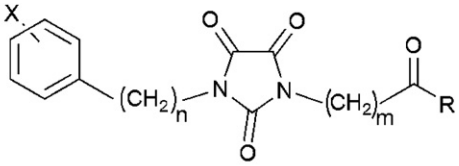

9 and **22-32**

Compound	X	n	m	R	Score	IC_{50} (μM)
TPI (4)	–	–	–	–	−70.1	0.036 ± 0.01[a]
18	H	1	–	–	−49.0	115 ± 8
19	2-Me	1	–	–	−51.4	128 ± 10
20	3-Cl	1	–	–	−52.9	117 ± 14
21	H	2	–	–	−48.6	103 ± 4
22	H	1	1	OEt	−58.3	342 ± 12
23	2-Me	1	1	OEt	−56.3	303 ± 17
24	3-Cl	1	1	OEt	−58.5	292 ± 43
25	H	2	1	OEt	−59.2	357 ± 25
26	H	1	1	OH	−69.1	264 ± 30
9	2-Me	1	1	OH	−72.2	236 ± 26
27	3-Cl	1	1	OH	−67.7	v. weak
28	H	2	1	OH	−69.3	85 ± 15
29	H	1	2	NH_2	−54.8	106 ± 13
30	2-Me	1	2	NH_2	−60.1	88 ± 10
31	3-Cl	1	2	NH_2	−54.4	66 ± 9
32	H	2	2	NH_2	−49.9	40 ± 6

[a] represents an upper limit for IC_{50} [11].

spectra were assigned with the aid of a ^{13}C DEPT NMR spectrum. Mass spectra were determined by the School of Chemistry, University of Manchester, using Micromass Trio 2000, chemical ionisation (CI), using NH_3 as an ionising gas. Electrospray (ES) mass spectra were recorded on a Micromass platform spectrometer using acetonitrile–water (1:1) as the mobile phase. Melting points were determined using a Gallenkamp MPD.350.BM2.5 instrument and remain uncorrected. Reactions were monitored using thin layer chromatography (TLC) on silica gel plates (precoated F_{254}, Merck 1.05554), spots were visualised using 254 nm UV light, $KMnO_4$ or

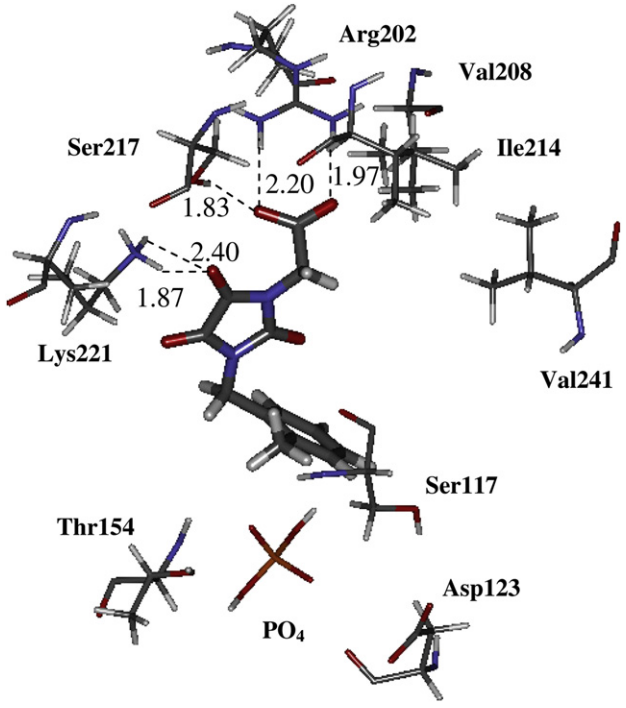

Fig. 4. The top-scoring pose of **9** in the active site of crystal structure of human TP. Distances are shown in Å.

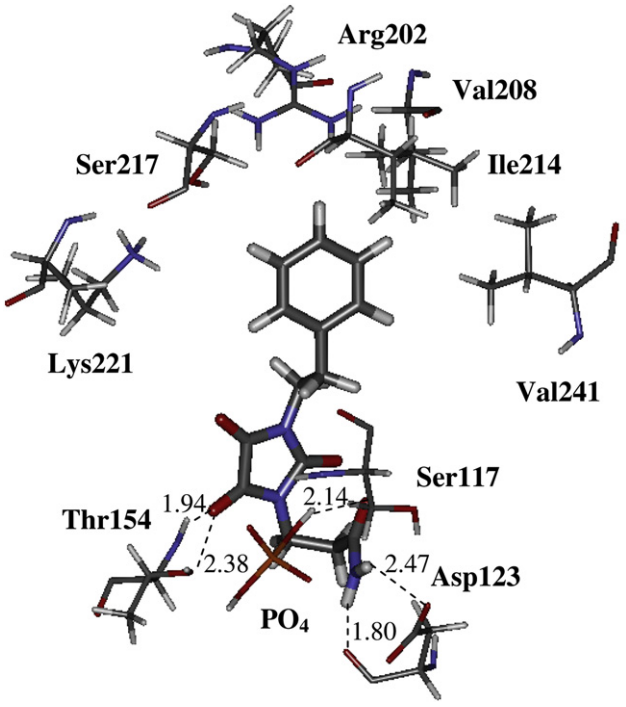

Fig. 5. The top-ranked pose of **32** in the active site of crystal structure of human TP. Distances are in Å.

DNP stain. Flash column chromatography was preformed using Prolabo silica gel 60 (35–75 μm particle size), 220–440 mesh. Solvents were distilled from the indicated drying agents, following standard procedures. Chemicals were obtained from The Aldrich Chemical Co., Dorset, UK. and Lancaster Synthesis LTD., Lancashire, UK. Enzyme rate spectral scans, studies of inhibition curves and absorbance readings at fixed wavelengths were conducted using a Peltier-thermostatted cuvette holder in a Cary 4000 UV–visible spectrophotometer equipped with Cary Enzyme Kinetics Software.

4.3. Synthesis

4.3.1. 1-Benzyl-imidazolidine-2,4,5-trione (**18**)

Trione **18** was prepared as described for **19** using benzylurea (**14**): colourless powder, yield: 88%. M.p. 168–171 °C; Lit. M.p. 169–170 °C [19]. IR (KBr) cm^{-1}: 3150 (NH), 1720 (C=O). ^1H NMR (DMSO-d_6) δ: 4.63 (2H, s, CH_2), 7.28–7.46 (5H, m, Ar–H), 12.10 (1H, s, NH). ^{13}C NMR (DMSO-d_6) δ: 41.8 (–CH_2–), 127.9 (C-4), 128.5 (C-2 and C-6), 129.3 (C-3 or C-5), 136 (C-1), 154.8 (C=O), 158.6 (C=O), 159.2 (C=O).

4.3.2. 1-(2-Methylbenzyl)-imidazolidine-2,4,5-trione (**19**)

Oxalyl chloride (0.10 ml, 1.2 mol) was added dropwise to a suspension of *N*-(2-methylbenzyl)urea (**15**) (0.164 g, 1 mmol) in tetrahydrofuran (3 ml) at 0 °C. The mixture was warmed to room temperature and stirred vigorously for 5 h. After removal of the precipitate by filtration, the filtrate was concentrated. The solid residue was dissolved in ethyl acetate (10 ml) and washed with water (2 × 10 ml) and then brine (10 ml). The organic layer was dried (anhydrous Na_2SO_4) and passed through a short silica gel pad. The solvent was evaporated. The solid was recrystallised from ethyl acetate–hexane to give **19** as colourless crystals (0.18 g, 82.5%). M.p. 192–194 °C; Lit. M.p. 195–196 °C [19]. IR (KBr) cm^{-1}: 3150 (NH), 1720 (C=O). ^1H NMR (DMSO-d_6) δ: 2.33 (3H, s, CH_3), 4.61 (2H, s, CH_2), 7.20–7.30 (4H, m, Ar–H), 12.10 (1H, s, NH). ^{13}C NMR (DMSO-d_6) δ: 19.1 (Ar–$\underline{C}H_3$), 40.4 (–CH_2–), 126.2 (C-5), 127.8 (C-4), 127.9 (C-6), 130.4 (C-3), 133.7 (C-2), 135.8 (C-1), 154.9 (C=O), 158.7 (C=O), 159.2 (C=O).

4.3.3. 1-(3-Chloro-benzyl)-imidazolidine-2,4,5-trione (**20**)

Trione **20** was prepared as described for **19** using 3-chlorobenzylurea (**16**): colourless powder, yield: 84%. M.p. 164–166 °C; Lit. M.p. 162–163 °C [19]. IR (KBr) cm^{-1}: 3210 (NH), 1720 (C=O). ^1H NMR (DMSO-d_6) δ: 4.65 (s, 2H, CH_2), 7.30–7.46 (m, 4H, Ar–H), 12.10 (s, 1H, NH). ^{13}C NMR (DMSO-d_6) δ: 46.4 (–CH_2–), 125.3 (C-6), 127.5 (C-4), 128.2 (C-2), 129.4 (C-5), 134.5 (C-3), 135.8 (C-1), 156.7 (C=O), 158.9 (C=O), 159.4 (C=O).

4.3.4. 1-Phenethyl-imidazolidine-2,4,5-trione (**21**)

Trione **21** was prepared as described for **19** using phenethylurea (**17**) (0.16 g, 1.0 mmol): colourless powder, yield: 96%. M.p. 189–192 °C; Lit. M.p. 189–190 °C [19]. IR (KBr) cm^{-1}: 3210 (NH), 1720 (C=O). ^1H NMR (DMSO-d_6) δ: 2.86 (2H, t, $^3J_{HH}$ = 7.6 Hz, Ph–CH_2), 3.66 (2H, t, $^3J_{HH}$ = 7.3 Hz, CH_2–N) 7.20–7.33 (5H, m, Phenyl), 12.10 (1H, s, NH). ^{13}C NMR (DMSO-d_6) δ: 32.9 (Ph–$\underline{C}H_2$), 39.7 (–$\underline{C}H_2$–N), 126.2 (C-4), 128.1 (C-2 and C-6), 128.2 (C-2 and C-5), 137.6 (C-1), 153.9 (C=O), 157.6 (C=O), 158.5 (C=O).

4.3.5. Ethyl (3-benzyl-2,4,5-trioxo-imidazolidin-1-yl)ethanoate (**22**)

The ester was prepared as described for **23** using trione **18**: colourless powder, yield: 89%. M.p. 147–150 °C, Lit. M.p. 150–151 °C [19]. IR (KBr, cm^{-1}): 1720 cm^{-1} (br, C=O). ^1H NMR (DMSO-d_6) δ: 1.20 (3H, t, $^3J_{HH}$ = 7.1 Hz, CH_3), 4.15 (2H, q, $^3J_{HH}$ = 7.1 Hz, OCH_2), 4.42 (2H, s, NCH_2CO_2), 4.75 (2H, s, Ph–CH_2), 7.30–7.39 (5H, m, Ph). ^{13}C NMR (DMSO-d_6) δ: 13.7 (CH_2–$\underline{C}H_3$), 40.1 (N–$\underline{C}H_2$), 42.3 (Ar–CH2–N), 61.4 ($O\underline{C}H_2$) 127.4 (C-4), 127.5 (C-2 and C-6), 128.3 (C-3 and C-5), 134.9 (C-1), 153.2 (C=O), 156.4 (C=O) and 156.6 (C=O, urea), 166.4 (C=O, ester).

4.3.6. Ethyl [3-(2-methyl-benzyl)-2,4,5-trioxo-imidazolidin-1-yl] ethanoate (**23**)

Trione **19** (0.22 g, 1 mmol) and ethyl bromoacetate (0.17 ml, 1.54 mmol) were added to a solution of potassium hydroxide (80 mg, 1.2 mmol) in ethanol (6 ml). After heating at reflux for 9 h, the mixture was cooled to 0 °C and filtered. The solid was dissolved in ethyl acetate (5 ml) and washed with water (15 ml) and brine (10 ml). The organic phase was dried (anhydrous Na_2SO_4) and passed through a short silica gel pad. After concentration, the crude solid was recrystallised from ethyl acetate–hexane to give **23** (0.24 g, 79%) as colourless crystals. M.p. 156–159 °C; Lit. M.p. 158–160 °C [19]. IR (KBr, cm^{-1}): 1720 cm^{-1} (br, C=O). ^1H NMR (DMSO-d_6) δ: 1.20 (3H, t, $^3J_{HH}$ = 7.1 Hz, CH_3), 2.34 (3H, s, Ar–$\underline{C}H_3$), 4.15 (2H, q, $^3J_{HH}$ = 7.1 Hz, OCH_2), 4.43 (2H, s, NCH_2CO_2), 4.73 (2H, s, Ar–CH_2), 7.13–7.26 (4H, m, Ar–H). ^{13}C NMR (DMSO-d_6) δ: 12.8 (Ar–$\underline{C}H_3$), 17.7 (CH_2–$\underline{C}H_3$), 39.8 (Ar–$\underline{C}H_2$), 40.5 (N$\underline{C}H_2$CO), 60.6 (O$\underline{C}H_2$) 124.9 (C-5), 126.5 (C-4), 126.6 (C-6), 129.1 (C-3), 131.9 (C-2), 134.6 (C-1), 152.4 (C=O), 155.5 (C=O) and 155.9 (C=O, amide), 166.0 (C=O, ester).

4.3.7. Ethyl [3-(3-chloro-benzyl)-2,4,5-trioxo-imidazolidin-1-yl] ethanoate (**24**)

The ester was prepared as described for **23** using trione **20** (0.24 g, 1.0 mmol): colourless powder, yield: 62%. M.p. 139–142 °C; Lit. M.p. 136–137 °C [19]. IR (KBr, cm^{-1}): 1720 (br, C=O). ^1H NMR (DMSO-d_6) δ: 1.19 (3H, t, $^3J_{HH}$ = 7.1 Hz, CH_3), 4.15 (2H, q, $^3J_{HH}$ = 7.1 Hz, OCH_2), 4.15 (2H, s, NCH_2CO_2), 4.76 (2H, s, Ar–CH_2), 7.30–7.45 (4H, m, Ar–H). ^{13}C NMR (DMSO-d_6) δ: 14.3 (CH_2–$\underline{C}H_3$), 40.0 (N–$\underline{C}H_2$), 41.7 (Ar–$\underline{C}H_2$), 62.0 (O$\underline{C}H_2$) 126.6 (C-6), 127.7 (C-4), 128.0 (C-2), 130.8 (C-5), 133.6 (C-3), 138.0 (C-1), 153.8 (C=O), 157.0 (C=O) and 157.2 (C=O), 167.0 (C=O, ester).

4.3.8. Ethyl (2,4,5-trioxo-3-phenethyl-imidazolidin-1-yl)ethanoate (**25**)

The ester **25** was prepared as described for **23** using trione **21**: colourless powder, yield: 85%. M.p. 106–110 °C; Lit. M.p. 106–108 °C [19]. IR (KBr, cm^{-1}): 1720 (br, C=O). ^1H NMR (DMSO-d_6) δ: 1.20 (3H, t, $^3J_{HH}$ = 7.1 Hz, CH_3), 2.89 (2H, t, $^3J_{HH}$ = 7.3 Hz, Ph–$\underline{C}H_2$), 3.77 (2H, t, $^3J_{HH}$ = 7.3 Hz, Ph–CH_2–$\underline{C}H_2$), 4.17 (2H, q, $^3J_{HH}$ = 7.1 Hz, OCH_2), 4.52 (2H, s, N–CH_2), 7.20–7.32 (5H, m, Ph). ^{13}C NMR (DMSO-d_6) δ: 13.8 ($\underline{C}H_3$), 33.0 (Ph–$\underline{C}H_2$), 39.6 (N–$\underline{C}H_2$), 40.2 (Ph–CH_2–$\underline{C}H_2$), 61.5 (O$\underline{C}H_2$), 126.5 (C-4), 128.4 (C-2 and C-6), 128.6 (C-3 and C-5), 137.5 (C-1), 153.2, 153.3 and 156.4 (C=O), 166.5 (C=O, ester).

4.3.9. (3-Benzyl-2,4,5-trioxo-imidazolidin-1-yl)ethanoic acid (**26**)

Acid **26** was prepared as described for **9** using **22**: colourless powder, yield: 69%. M.p. 203–208 °C, Lit. M.p. 207.5–209.5 °C [19]. IR (KBr, cm^{-1}): 3200–2800 cm^{-1} (br, CO_2H), 1710 cm^{-1} (br, C=O). ^1H NMR (DMSO-d_6) δ: 4.22 (2H, s, N–CH_2), 4.74 (2H, s, Ph–$\underline{C}H_2$), 7.26–7.39 (5H, m, Ph), 13.2 (1H, br s, OH). ^{13}C NMR (DMSO-d_6) δ: 40.6 (Ph–$\underline{C}H_2$ or N–CH_2), 41.5 (Ph–$\underline{C}H_2$ or N–CH_2), 125.7 (C-4), 126.3 (C-2 and C-6), 127.3 (C-3 and C-5), 133.9 (C-1), 152.2 (C=O), 155.4 (C=O), 155.6 (C=O), 166.7 (C=O, $\underline{C}OOH$).

4.3.10. [3-(2-Methylbenzyl)-2,4,5-trioxo-imidazolidin-1-yl] ethanoic acid (**9**)

A mixture of **23** (0.20 g, 0.66 mmol), acetic acid (0.6 ml) and concentrated hydrochloric acid (0.3 ml) was heated at reflux for 3 h. The reaction mixture was concentrated under reduced pressure to give a residue, which was heated at reflux with acetic acid (0.6 ml) and concentrated hydrochloric acid (0.3 ml) for a further 2 h. The

solid obtained by concentration was dissolved in ethyl acetate, washed with water, and extracted with 10% aqueous sodium carbonate. The aqueous layer was washed with ethyl acetate and acidified with concentrated hydrochloric acid. The precipitated solid was extracted with ethyl acetate, washed with water and brine, and dried (anhydrous Na_2SO_4). Concentration followed by crystallisation from diethyl ether gave **9** as a cream solid (0.12 g, 65%). M.p. 193–196 °C; Lit. M.p. 198–199 °C [19]. IR (KBr, cm^{-1}): 3200–2800 cm^{-1} (br, CO_2H), 1710 cm^{-1} (br, C=O). ^1H NMR (DMSO-d_6) δ: 2.35 (3H, s, CH_3), 4.31 (2H, s, N–CH_2), 4.73 (2H, s, Ar–CH_2), 7.13–7.26 (4H, m, Ar–H), 13.5 (1H, br s, OH). ^{13}C NMR (DMSO-d_6) δ: 19.1 (CH_3), 40.1 (Ar–CH_2), 40.4 (NCH_2CO_2), 126.3 (C-5), 128.0 (C-4), 128.1 (C-6), 130.5 (C-3), 133.3 (C-2), 136.1(C-1), 154.0 (C=O), 157.0 (C=O), 157.4 (C=O), 168.4 (COOH).

4.3.11. [3-(3-chloro-benzyl)-2,4,5-trioxo-imidazolidin-1-yl] ethanoic acid (**27**)

Acid **27** was prepared as described for **9** using **24**: colourless powder, yield: 87%. M.p. 210–214 °C, Lit. M.p. 207–208 °C [19]. IR (KBr, cm^{-1}): 3200–2800 cm^{-1} (br, CO_2H), 1710 cm^{-1} (br, C=O). ^1H NMR (DMSO-d_6) δ: 4.30 (2H, s, N–CH_2), 4.77 (2H, s, Ar–CH_2), 7.22–7.44 (4H, m, Ar–H), 12.9 (1H, br s, OH). ^{13}C NMR (DMSO-d_6) δ: 40.7 (Ar–CH_2 or N–CH_2), 41.7 (Ar–CH_2 or N–CH_2), 126.6 (C-6), 127.7 (C-4), 128.1 (C-2), 130.8 (C-5), 133.6 (C-3), 138.0 (C-1), 153.8 (C=O), 157.1 (C=O), 157.3 (C=O), 168.3 (COOH).

4.3.12. (2,4,5-Trioxo-3-phenethyl-imidazolidin-1-yl)ethanoic acid (**28**)

Acid **28** was prepared as described for **9** using **25**: colourless powder, yield: 76%. M.p. 153–155 °C, Lit. M.p. 154.5–155.5 °C [19]. IR (KBr, cm^{-1}): 3200–2800 cm^{-1} (br, CO_2H), 1710 cm^{-1} (br, C=O). ^1H NMR (DMSO-d_6) δ:2.90 (2H, t, $^3J_{HH}$ = 7.2 Hz, Ph–CH_2), 3.78 (2H, t, $^3J_{HH}$ = 7.1 Hz, CH_2–N), 4.30 (2H, s, CH_2–CO), 7.24–7.39 (5H, m, Ph), 12.8 (1H, br s, OH). ^{13}C NMR (DMSO-d_6) δ: 32.4 (Ar–CH_2), 43.2 (Ar–CH2–CH_2), 46.8 (NCH_2CO_2), 124.3 (C-4), 129.3 (C-2 and C-6), 131.6 (C-3 and C-5), 135.6 (C-1), 158.1, 158.3 and 159.2 (C=O), 166.9 (COOH).

4.3.13. 3-(3-Benzyl-2,4,5-trioxo-imidazolidin-1-yl)-propionamide (**29**)

Amide **29** was prepared as described for **30** using **18**: colourless powder, yield: 72%. M.p. 201–203 °C. Anal. Calc. for $C_{13}H_{13}N_3O_4$: 56.71% C, 4.76% H, N 15.27%; found 56.50% C, 4.11% H, 14.51% N. IR (KBr) cm^{-1}: 3200–3500 (NH_2), 1720 (C=O), 1660 (C=O), 1630 (C=O). ^1H NMR (DMSO-d_6) δ: 2.40 (2H, t, $^3J_{HH}$ = 7.6 Hz, CH_2CO), 3.68 (2H, t, $^3J_{HH}$ = 7.6 Hz, N–CH_2), 4.61 (2H, s, Ar–CH_2), 6.90 (1H, br s, NH), 7.30–7.35 (5H, m, Ph), 7.45 (1H, br s, NH). ^{13}C NMR (DMSO-d_6) δ: 34.5 (CH_2CONH_2), 38.8 (NCH_2CH_2), 48.2 (Ph–CH_2), 126.7 (C-4), 127.3 (C-2/6), 127.8 (C-3/5), 139.6 (C-1), 156.2 (C=O), 156.9 (C=O), 157.7 (C=O), 173.2 ($CONH_2$). MS (ES+): 298 ([M + Na]$^+$, 100%).

4.3.14. 3-(2-Methylbenzyl)-2,4,5-trioxoimidazolidin-1-yl-propionamide (**30**)

A mixture of **19** (0.22 g, 1 mmol) and 3-bromopropionamide [27] (0.23 g, 1.54 mmol) was added to a solution of KOH (80 mg, 1.2 mmol) in ethanol (6 ml). After heating at reflux for 8 h, the mixture was cooled to 0 °C and filtered. The solid was dissolved in ethyl acetate and washed with water (10 ml) and brine (10 ml). The organic phase was dried over (anhydrous Na_2SO_4) and passed through a short silica gel pad. After being concentrated, the crude solid was recrystallised from ethyl acetate–hexane to give (**30**) (0.26 g, 90%) as colourless crystals. M.p. 199–201 °C. Anal. Calc. for $C_{14}H_{15}N_3O_4$: 58.13% C, 5.23% H; found: 58.27% C, 4.91% H. IR (KBr) cm^{-1}: 3200–3500 (NH_2), 1720 (C=O), 1660 (C=O), 1630 (C=O). ^1H NMR (DMSO-d_6), δ: 2.34 (3H, s, CH_3), 2.42 (2H, t, $^3J_{HH}$ = 7.6 Hz, CH_2CO), 3.70 (2H, t, $^3J_{HH}$ = 7.6 Hz, N–CH_2), 4.61 (2H, s, Ar–CH_2), 6.90 (1H, br s, NH), 7.28–7.35 (4H, m, Ar–H), 7.39 (1H, br s, NH). ^{13}C NMR (DMSO-d_6), δ: 19.1 (Ar–CH_3), 33.2 (CH_2CONH_2), 35.5 (NCH_2CH_2), 40.2 (Ar–CH_2), 126.2 (C-5), 127.8 (C-4), 127.9 (C-6), 130.4 (C-3), 133.7 (C-2), 135.8 (C-1), 154.9 (C=O), 155.2 (C=O), 158.7 (C=O), 171.6 ($CONH_2$). MS (ES+): 312 ([M + Na]$^+$, 100%), 307 ([M + NH_4]$^+$, 50%). Accurate mass 290.1138. $C_{14}H_{16}N_3O_4$ (M + H) requires 290.1135.

4.3.15. 3-[3-(3-Chlorobenzyl)-2,4,5-trioxo-imidazolidin-1-yl]-propionamide (**31**)

Amide **31** was prepared as described for **30** using **20**: colourless powder, yield: 38%. M.p. 218–221 °C. Anal. Calc. for $C_{13}H_{12}ClN_3O_4$: 50.42% C, 3.91% H, 13.57% N, 11.45% Cl; found: 50.19% C, 3.82% H, 13.11% N, 11.16% Cl. IR (KBr) cm^{-1}: 3200–3500 (NH_2), 1720 (C=O), 1660 (C=O), 1630 (C=O). ^1H NMR (DMSO-d_6), δ: 2.48 (2H, t, $^3J_{HH}$ = 7.6 Hz, CH_2CO), 3.70 (2H, t, $^3J_{HH}$ = 7.6 Hz, N–CH_2), 4.61 (2H, s, Ar–CH_2), 6.90 (1H, br s, NH), 7.34–7.38 (4H, m, Ar–H), 7.46 (1H, br s, NH). ^{13}C NMR (DMSO-d_6), δ: 39.8 (CH_2CONH_2), 40.1 (NCH_2CH_2), 49.3 (Ar–CH_2), 126.4 (C-6), 127.1 (C-4), 127.8 (C-2), 128.8 (C-5), 134.2 (C-3), 138.9(C-1), 155.2 (C=O), 155.8 (C=O), 156.3 (C=O), 176.5 ($CONH_2$). MS(ES+): 332 (^{35}Cl [M + Na]$^+$, 100%), 334 (^{37}Cl [M + Na]$^+$, 30%). MS(ES-): 308 (^{35}Cl M–H, 100%), 310 (^{37}Cl M–H, 30%).

4.3.16. 3-(2,4,5-Trioxo-3-phenethyl-imidazolidin-1-yl)-propionamide (**32**)

Amide **32** was prepared as described for **30** using **21**: colourless powder, yield: 96%. M.p. 146–149 °C. Anal. Calc. for $C_{14}H_{15}N_3O_4$: 58.11% C, 5.23% H, N 14.53% N; found: 57.77% C, 5.21% H, 13.54% N. IR (KBr) cm^{-1}: 3200–3500 (NH_2), 1720 (C=O), 1660 (C=O), 1630 (C=O). ^1H NMR (DMSO-d_6) δ: 2.48 (2H, t, $^3J_{HH}$ = 7.6 Hz, CH_2CO), 2.93 (2H, t, $^3J_{HH}$ = 7.6 Hz, Ph–CH_2), 3.70 (2H, t, $^3J_{HH}$ = 7.6 Hz, N–CH_2 or CH_2–N), 3.72 (2H, t, $^3J_{HH}$ = 7.6 Hz, N–CH_2 or CH_2–N), 6.91 (1H, br s, NH), 7.22–7.33 (5H, m, Ph), 7.44 (1H, br s, NH). ^{13}C NMR (DMSO-d_6) δ: 36.4 (Ph–CH_2), 36.9 (CH_2CONH_2), 42.3 (NCH_2CH_2), 49.3 (–CH_2–N), 126.3 (C-4), 127.6 (C-2 and C-6), 128.3 (C-3 and C-5), 139.7 (C-1), 158.2 (C=O), 158.8 (C=O), 159.4 (C=O), 169.4 ($CONH_2$). MS (ES+): 312 ([M + Na]$^+$, 100%).

4.4. TP inhibition assay

The 1 ml assay mix contained 20 μM thymidine, 0.1 M potassium phosphate buffer (pH 7.4), together with the TP inhibitor. The reaction was initiated by addition of *E. coli* TP enzyme (0.22 units) and the change in absorbance was monitored at 265 nm at 25 °C [11,20]. Enzyme kinetics data were analysed using Grafit version 3 software (Erithacus software).

Acknowledgements

We thank the School of Pharmacy for partial funding (MR), COST 606 and EPSRC for studentship and PhD plus fellowship (DM). We thank Waleed Zalloum for assistance in preparation of figures and Philip N. Edwards (p.n.e@btinternet.com) for informative and challenging discussions.

References

[1] T.A. Krenitsky, G.W. Koszalka, J.V. Tuttle, Purine nucleoside synthesis: an efficient method employing nucleoside phosphorylases, Biochemistry 20 (1981) 3615–3621.
[2] M. Haraguchi, K. Miyadera, K. Uemura, T. Sumizawa, T. Furukawa, K. Yamada, S.-I. Akiyama, Y. Yamada, Angiogenic activity of enzymes, Nature 368 (1994) 198.
[3] K. Miyadera, T. Sumizawa, M. Haraguchi, H. Yoshida, W. Konstanty, Y. Yamada, S.-I. Akiyama, Role of thymidine phosphorylase activity in the angiogenic effect of platelet-derived endothelial cell growth factor/thymidine phosphorylase, Cancer Res. 55 (1995) 1687–1690.

[4] E.J. Yu, Y. Lee, S.Y. Rha, T.S. Kim, H.C. Chung, B.K. Oh, W.I. Yang, S.H. Noh, H.-C. Jeung, Angiogenic factor thymidine phosphorylase increases cancer cell invasion activity in patients with gastric adenocarcinoma, Mol. Cancer Res. 6 (2008) 1554–1566.
[5] A. Bronckaers, F. Gago, J. Balzarini, S. Liekens, The dual role of thymidine phosphorylase in cancer development and chemotherapy, Med. Res. Rev. 29 (2009) 903–953.
[6] M. de Bruin, T. van Capel, K. Smid, K. van der Born, M. Fukushima, K. Hoekman, H.M. Pinedo, G.J. Peters, Role of platelet derived endothelial cell growth factor/thymidine phosphorylase in fluoropyrimidine sensitivity and potential role of deoxyribose-1-phosphate, Nucleos. Nucleot. Nucl. Acids 23 (2004) 1485–1490.
[7] R. Ikeda, X.-F. Che, M. Ushiyama, T. Yamaguchi, H. Okumura, Y. Nakajima, Y. Takeda, Y. Shibayama, T. Furukawa, M. Yamamoto, M. Haraguchi, T. Sumizawa, K. Yamada, S.-I. Akiyama, 2-Deoxy-D-ribose inhibits hypoxia-induced apoptosis by suppressing the phosphorylation of p38 MAPK, Biochem. Biophys. Res. Commun. 342 (2006) 280–285.
[8] S. Matsushita, T. Nitanda, T. Furukawa, T. Sumizawa, A. Tani, K. Nishimoto, S. Akiba, K. Miyadera, M. Fukushima, Y. Yamada, H. Yoshida, T. Kanzaki, S.-I. Akiyama, The effect of a thymidine phosphorylase inhibitor on angiogenesis and apoptosis in tumors, Cancer Res. 59 (1999) 1911–1916.
[9] C. Cole, P. Reigan, A. Gbaj, P.N. Edwards, K.T. Douglas, I.J. Stratford, S. Freeman, M. Jaffar, Potential tumor-selective nitroimidazolylmethyluracil prodrug derivatives: inhibitors of the angiogenic enzyme thymidine phosphorylase, J. Med. Chem. 46 (2002) 207–209.
[10] P. Reigan, A. Gbaj, E. Chinje, I.J. Stratford, K.T. Douglas, S. Freeman, Synthesis and enzymatic evaluation of xanthine oxidase-activated prodrugs based on inhibitors of thymidine phosphorylase, Bioorg. Med. Chem. Lett. 14 (2004) 5247–5250.
[11] P. Reigan, P.N. Edwards, A. Gbaj, C. Cole, S.T. Barry, K.M. Page, S.E. Ashton, R.W.A. Luke, K.T. Douglas, I.J. Stratford, M. Jaffar, R.A. Bryce, S. Freeman, Aminoimidazolylmethyluracil analogues as potent inhibitors of thymidine phosphorylase and their bioreductive nitroimidazolyl prodrugs, J. Med. Chem. 48 (2005) 392–402.
[12] M.P. Price, W. Guida, T. Jackson, J. Nydick, P. Gladstone, J. Juarez, F. Donate, R. Ternansky, Design of novel *N*-(2,4-dioxo-1,2,3,4-tetrahydro-thieno[3,2-d] pyrimidin-7-yl)-guanidines as thymidine phosphorylase inhibitors, and flexible docking to a homology model, Bioorg. Med. Chem. Lett. 13 (2003) 107–110.
[13] V.A. McNally, A. Gbaj, K.T. Douglas, I.J. Stratford, M. Jaffar, S. Freeman, R.A. Bryce, Identification of a novel class of inhibitor of human and *Escherichia coli* thymidine phosphorylase by *in silico* screening, Bioorg. Med. Chem. Lett. 13 (2003) 3705–3709.
[14] M. Rajabi. Design, synthesis and biological evaluation of thymidine phosphorylase inhibitors as anti-cancer drugs, PhD Thesis (2007), The University of Manchester.
[15] R.A. Norman, S.T. Barry, M. Bate, J. Breed, J.G. Colls, R.J. Ernill, R.W.A. Luke, C.A. Minshull, M.S.B. McAlister, E.J. McCall, H.H.J. McMiken, D.S. Paterson, D. Timms, J.A. Tucker, R.A. Pauptit, Crystal structure of human thymidine phosphorylase in complex with a small molecule inhibitor, Structure 12 (2004) 75–84.
[16] P.F. Kador, J.H. Kinoshita, N.E. Sharpless, Aldose reductase inhibitors: a potential new class of agents for the pharmacological control of certain diabetic complications, J. Med. Chem. 28 (1985) 841–849.
[17] P.F. Kador, W.G. Robison, J.H. Kinoshita, The pharmacology of aldose reductase inhibitors, Annu. Rev. Pharmacol. Toxicol. 25 (1985) 691–714.
[18] P.F. Kador, The role of aldose reductase in the development of diabetic complications, Med. Res. Rev. 8 (1988) 325–352.
[19] A. Ishii, T. Kotani, Y. Nagaki, Y. Shibayama, Y. Toyomaki, N. Okukado, K. Ienaga, K. Okamoto, Highly selective aldose reductase inhibitors. 1. 3-(Arylalkyl)-2,4,5-trioxoimidazolidine-1-acetic acids, J. Med. Chem. 39 (1996) 1924–1927.
[20] C. Nakayama, Y. Wataya, R.B. Meyer Jr., D.V. Santi, M. Saneyoshi, T. Ueda, Thymidine phosphorylase. Substrate specificity for 5-substituted 2′-deoxyuridines, J. Med. Chem. 23 (1980) 962–964.
[21] J. Balzarini, A.E. Gamboa, R. Esnouf, S. Liekens, J. Neyts, E.D. Clercq, M.-J. Camarasa, M.-J. Pérez-Pérez, 7-Deazaxanthine, a novel prototype inhibitor of thymidine phosphorylase, FEBS Lett 438 (1998) 91–95.
[22] M.J. Pugmire, S.E. Ealick, The crystal structure of pyrimidine nucleoside phosphorylase in a closed conformation, Structure 6 (1998) 1467–1479.
[23] T.J.A. Ewing, S. Makino, A.G. Skillman, I.D. Kuntz, DOCK 4.0: search strategies for automated molecular docking of flexible molecule databases, J. Comput. Aid. Mol. Des 15 (2001) 411–428.
[24] J. Gasteiger, M. Marsili, Iterative partial equalization of orbital electronegativity: a rapid access to atomic charges, Tetrahedron 36 (1980) 3219–3222.
[25] T.A. Halgren, Merck molecular force field. I. Basis, form, scope, parameterization, and performance of MMFF94, J. Comput. Chem. 17 (1996) 490–519.
[26] M.L. Verdonk, J.C. Cole, M.J. Hartshorn, C.W. Murray, R.D. Taylor, Improved protein-ligand docking using GOLD, Proteins: Struct. Funct. Genet. 52 (2003) 609–623.
[27] D.D. Tanner, C.P. Meintzer, Reexamination of the reaction of a “graded set” of radicals with *N*-bromosuccinimide: a kinetic argument concerning the π and σ states of succinimidyl, J. Am. Chem. Soc. 107 (1985) 6584–6589.